

# Improved Performance of Protected Catecholic Polysiloxanes for Bioinspired Wet Adhesion to Surface Oxides

Jinhwa Heo,<sup>†,‡,○</sup> Taegon Kang,<sup>†,‡,○</sup> Se Gyu Jang,<sup>†</sup> Dong Soo Hwang,<sup>‡</sup> Jason M. Spruell,<sup>†</sup> Kato L. Killops,<sup>#</sup> J. Herbert Waite,<sup>†,§,||</sup> and Craig J. Hawker<sup>\*,†,‡,§,∇</sup>

<sup>†</sup>Materials Research Laboratory, <sup>‡</sup>Materials Department, <sup>§</sup>Department of Chemistry and Biochemistry, and <sup>||</sup>Department of Molecular, Cell & Developmental Biology, University of California, Santa Barbara, California 93106, United States

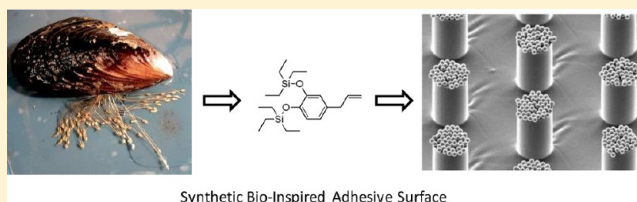
<sup>‡</sup>Ocean Science and Technology Institute, Pohang University of Science and Technology, Pohang 790-784, Republic of Korea

<sup>#</sup>Edgewood Chemical Biological Center, U.S. Army Research, Development, and Engineering Command, Aberdeen Proving Ground, Maryland 21010, United States

<sup>∇</sup>Center for Refining & Petrochemicals, King Fahd University of Petroleum and Minerals, Dhahran, Saudi Arabia 31261

## S Supporting Information

**ABSTRACT:** A facile synthetic strategy for introducing catecholic moieties into polymeric materials based on a readily available precursor (eugenol) and efficient chemistries [tris-(pentafluorophenyl)borane-catalyzed silylation and thiol–ene coupling] is reported. Silyl protection is shown to be critical for the oxidative stability of catecholic moieties during synthesis and processing, which allows functionalized polysiloxane derivatives to be fabricated into 3D microstructures as well as 2D patterned surfaces. Deprotection gives stable catechol surfaces whose adhesion to a variety of oxide surfaces can be precisely tuned by the level of catechol incorporation. The advantage of silyl protection for catechol-functionalized polysiloxanes is demonstrated and represents a promising and versatile new platform for underwater surface treatments.



Synthetic Bio-Inspired Adhesive Surface

## INTRODUCTION

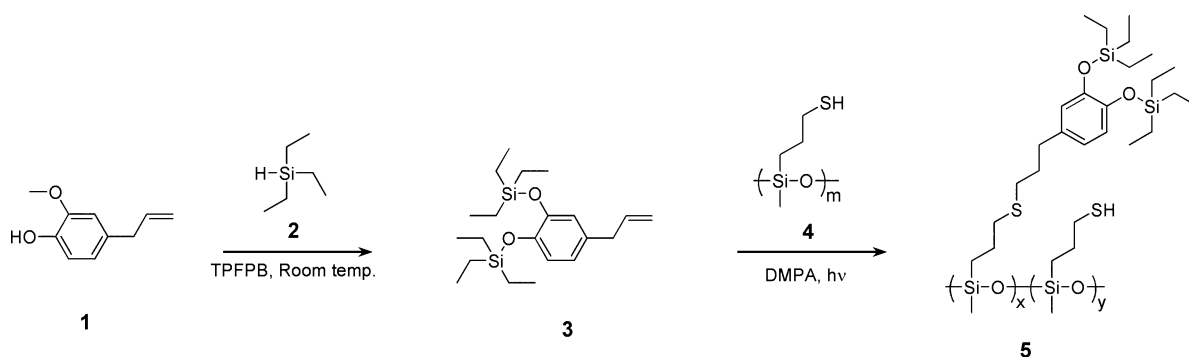
The harsh aqueous environments endured by different marine species have inspired the development of a range of synthetic materials based on the functional groups/nanostructures<sup>1,2</sup> and assembly processes<sup>3,4</sup> present in the natural systems. This is especially true for adhesive proteins derived from marine fouling organisms (e.g., mussels, hydroids, and tubeworms), which have attracted considerable interest because of their rapid and strong binding to nearly all surfaces.<sup>5–7</sup> A key chemical functionality present in the adhesive proteins of mussels and sandcastle worms is the amino acid 3,4-dihydroxy-L-phenylalanine (DOPA),<sup>8,9</sup> the catecholic moiety of which has an attractive and diverse range of chemistries, including (a) the formation of strong coordination complexes with diverse metal ions, (b) the ability to undergo covalent cross-linking, (c) rich oxidation/reduction chemistry, and (d) a variety of energetic surface interactions.<sup>10–14</sup> Mussels appear to have spatial control over all four of the above features within their adhesives,<sup>11,15–17</sup> but with the exception of adhesion to living tissues, most efforts using synthetic catechol-functionalized polymers have been stymied by the oxidative instability of unprotected catechols in the neutral to basic pH range. Our goal was to develop a strategy that overcomes this instability, thereby enabling the preparation of a diverse range of two-dimensional (2D) and three-dimensional (3D) features for demanding underwater applications.

Synthetically, the strategy relies upon the preparation of catechol-functionalized polyorganosiloxanes (alternatively called silicones or polysiloxanes) from readily available building blocks that are designed to serve as broadly applicable and cross-linkable artificial adhesives. Silicones, as a general class of materials, are ubiquitous in technology, with applications ranging widely from electrical materials to biomaterials as a result of their unique properties, such as low glass transition temperatures, low surface energies, transparency, good thermal and oxidative stability, low moduli, high flexibility, and excellent moldability.<sup>18–23</sup> Although polysiloxanes are capable of molding and patterning as cross-linked microstructures, their inherently low mechanical and antiadhesive properties, as well as side reactions that occur during traditional thermal curing processes, pose complications for their use as catechol-based wet adhesive materials. Lee and co-workers reported polysiloxane structural pillars having wet/dry adhesiveness resulting from a coating of an adhesive polymer onto prefabricated polysiloxane pillars inspired by gecko and mussel<sup>24</sup> biological nanostructures. While this method forms polysiloxane arrays that are useful for a reversible wet/dry adhesive, it is costly and complicated, requiring the formation of nanostructured polysiloxanes through electron-beam lithography followed by coating with underwater adhesive polymers. Of particular note

Received: September 11, 2012

Published: November 26, 2012

**Scheme 1. Synthesis of Silyl-Protected Catecholic Derivative 3 and Reactive Silyl-Protected Catechol (SPC)-Functionalized Polysiloxane Building Block 5**



is the care that must be taken to prevent catechol oxidation, which significantly undermines the polymer adhesion.<sup>25,26</sup>

Our strategy overcomes these issues by employing a common building block, eugenol (the active ingredient of clove oil, which is readily available in large quantities), and two efficient and orthogonal reactions, namely, tris-(pentafluorophenyl)borane (TPFPB)-catalyzed silylation and thiol–ene coupling, to prepare adhesive catechol-functionalized polysiloxanes. In turn, this new class of marine-inspired adhesive polysiloxanes has a number of advantages, including ease of synthesis, versatility, and inherent stability, with the resulting air- and moisture-stable materials being activated through a simple deprotection process. The first enabler in our strategy, the TFPFB-catalyzed silylation, has been used for hydrosilylation of various nucleophilic groups,<sup>27–35</sup> including ethers, and is highly efficient and insensitive to moisture.<sup>36–38</sup> Moreover, the orthogonal reactivity of TFPFB allows the facile one-step transformation of eugenol into a reactive, bis-silyl-protected DOPA mimic. The silyl protecting groups are key to maintaining the stability of the catechol unit throughout the thiol–ene polymer functionalization, processing, and subsequent cross-linking reactions. Moreover, these silyl protecting groups serve to provide a long shelf life to the assembled materials but can be selectively removed under mild acidic or basic conditions, such as during conventional contact printing strategies, essentially activating the adhesive properties just prior to use.

The second enabler is the thiol–ene reaction, which allows the attachment of the protected eugenol moieties to the polymer backbone. Significantly, this reaction proceeds in high yields with tolerance for various functional groups even under solvent-free conditions, and it has been widely used for the modification of polymers,<sup>39–44</sup> thin-film fabrication,<sup>45–47</sup> and dendrimer synthesis.<sup>39,48,49</sup> Because of its high efficiency and simplicity, the thiol–ene reaction is an ideal partner for quantitative functionalization of the siloxane backbone and subsequent preparation of thin films and functionalized polymers.<sup>50–52</sup>

Herein we demonstrate the preparation of novel bioinspired polysiloxanes with controlled catechol functional group incorporation through facile and efficient chemistry. These building blocks are then used to fabricate 3D microstructures with tunable adhesion and high stability due to the suppression of oxidative side reactions of the key catechol units.

## RESULTS AND DISCUSSION

The investigation of marine organisms has provided insights into the design criteria needed for the preparation of synthetic underwater adhesive polymers. First of all, the synthetic materials should have unoxidized catecholic moieties for adhesion, and the concentration of catecholic moieties should be adjustable to mimic the various adhesive proteins of marine organisms and, conversely, various potential applications. Second, facile fabrication strategies for both surface modification and the construction of 3D microstructures are highly desirable. In addition, minimal loss of material through solubilization in the surrounding aqueous solution is required for the molded structures to endure, necessitating a degree of hydrophobicity. Lastly, simple protection and deprotection methods are desired to prevent premature oxidation of the catecholic moieties during synthesis and storage of the synthetic adhesive materials. Traditionally, during synthesis and processing catecholic units are prone to be oxidized to *o*-quinone groups, which then undergo secondary reactions with nucleophiles such as amines, thiols, and other catechols, causing extensive cross-linking and aggregation that result in reduced adhesion and poor performance. To address these challenges, silyl-protected catechol (SPC)-functionalized polysiloxanes, employing eugenol as a naturally derived and economically viable precursor, were prepared, and their fabrication into thin films and microstructures was studied.

The synthetic strategy for the key silyl-protected catecholic intermediate, 3, and the corresponding SPC-functionalized polysiloxane, 5, is illustrated in Scheme 1. Hydrosilylation of both the phenolic and methyl ether units of eugenol (1) was achieved through a one-pot transformation catalyzed by TFPFB in the presence of triethylsilane (2). The reaction of 1 and 2 proved to be facile at room temperature under ambient conditions, with complete consumption of starting materials occurring within 10 min. The crude silyl-protected derivative 3 was then filtered through neutral alumina to remove the TFPFB, giving 3 as a pure product in quantitative yield without any need for further purification. Auspiciously, 3 retains the terminal alkene group of 1, which can be used as a reactive handle for attachment to a wide variety of polymer backbones through thiol–ene chemistry. With commercially available poly[(mercaptopropyl)methylsiloxane] (PMMS, 4) (Scheme 1) as the thiol-functionalized siloxane precursor, polymers functionalized with SPC units could be routinely prepared with varying levels of SPC incorporation (5–50 mol %). Because of the facile nature of this chemistry, photoirradiation of a neat mixture of 4, varying mole percentages of silyl-protected

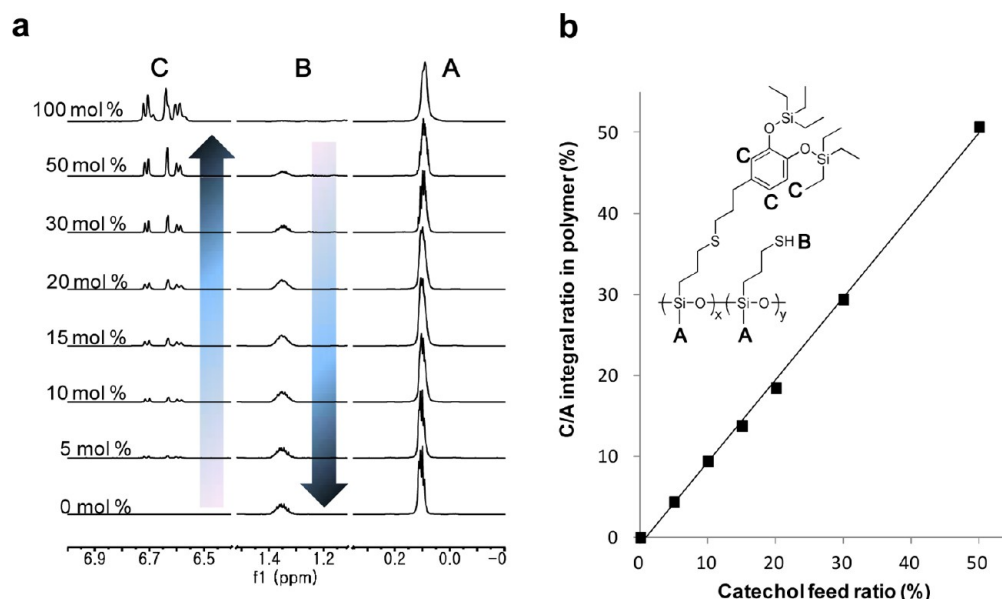


**Figure 1.** Characterization of the level of catechol incorporation for the SPC-functionalized polysiloxanes. (a) <sup>1</sup>H NMR spectra of SPC-functionalized polysiloxanes with different mole percentages of silyl-protected catecholic units attached. All of the spectra were normalized to the intensity of the Si methyl resonance at ca. 0.1 ppm. (b) Plot of the catechol/Si methyl (C/A) <sup>1</sup>H NMR integral ratio vs the catechol/thiol repeat unit feed ratio.

catechol **3**, and 2,2-dimethoxy-2-phenylacetophenone (DMPA) at room temperature for 30 min resulted in quantitative incorporation of the protected catechol, allowing the percent SPC incorporation to be controlled simply by varying the ene/thiol feed ratio (Figure 1b). It should be noted that all of the SPC-functionalized polymers were stable and could be kept under ambient conditions for weeks or stored at 0 °C for months without any observable degradation.

Figure 1a displays the <sup>1</sup>H NMR spectra for a series of SPC-functionalized polysiloxanes, which clearly exhibited unique resonances for each repeat unit that allowed the calculation of the percent incorporation of the SPC units as a function of the feed ratio. While the PMMS backbone could be fully functionalized with catecholic units (100 mol %), the highest loading used for this study was 50 mol %. In comparison, naturally occurring mussel foot protein 5 (mfp-5) of the *Mytilus* genus, which contains the highest DOPA loading found in nature, has a ~30 mol % loading of DOPA units along the backbone.<sup>53</sup> From a total catechol concentration viewpoint, the polymers in this study are therefore good analogues of those employed by a wide range of marine organisms. Indeed, there are no other reports of polymers functionalized with catecholic moieties to 50 mol % levels, presumably because of oxidative instability and uncontrolled cross-linking. Notably, the silyl protecting groups were stable throughout the synthesis and handling of these materials (as indicated by the resonances at 0.98 and 0.74 ppm in the <sup>1</sup>H NMR spectra), and their presence ensured that the catechol groups would not participate in any undesirable, premature adhesion and would be stable toward unwanted side reactions involving oxidative pathways.

The availability of SPC-functionalized polysiloxanes bearing both protected catechol and unreacted thiol groups presents a stable and highly functional platform for the fabrication of cross-linked microstructures. We were particularly interested in the generation of micropillar arrays using imprint lithography and the measurement of adhesive forces with a modified atomic force microscopy (AFM) strategy. A liquid prepolymer mixture

of the SPC-functionalized PMMS **5**, triallyl cyanurate (TAC), dimethacrylate of ethoxylated bisphenol A (BPADMA), and DMPA was therefore applied to a patterned soft-imprint mold and cured through UV irradiation ( $\lambda = 365$  nm, 4.6 mW cm<sup>-2</sup>) for 4 min under ambient conditions (Figure 2b). This soft mold

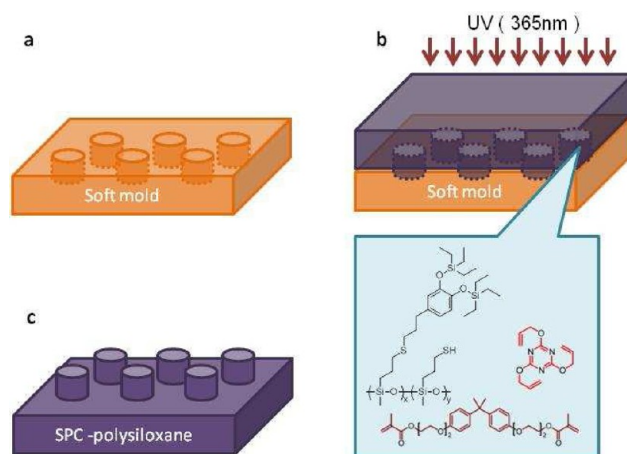


**Figure 2.** Process for fabrication of microstructures using SPC-functionalized polysiloxane and imprint lithography. (a) Fabrication of the soft-imprint mold. (b) Casting of a mixture of SPC-functionalized polysiloxane and alkene cross-linkers onto the patterned soft-imprint mold with subsequent photocuring. (c) Removal of the mold to give SPC-functionalized polysiloxane-based microstructures.

was prepared from a hard Si master through soft-imprint lithography methods using thiol–ene chemistry<sup>50</sup> (see Supplementary Figure S2 in the Supporting Information). The photocured SPC-functionalized polysiloxane-based replica film was then easily peeled from the soft mold. To ensure that a uniform contact area would be measured in each case, the pillars were designed with dimensions smaller than the contact area of the tipless AFM cantilever (100  $\mu$ m length  $\times$  13.5  $\mu$ m width) and with sufficient spacing between pillars to ensure that

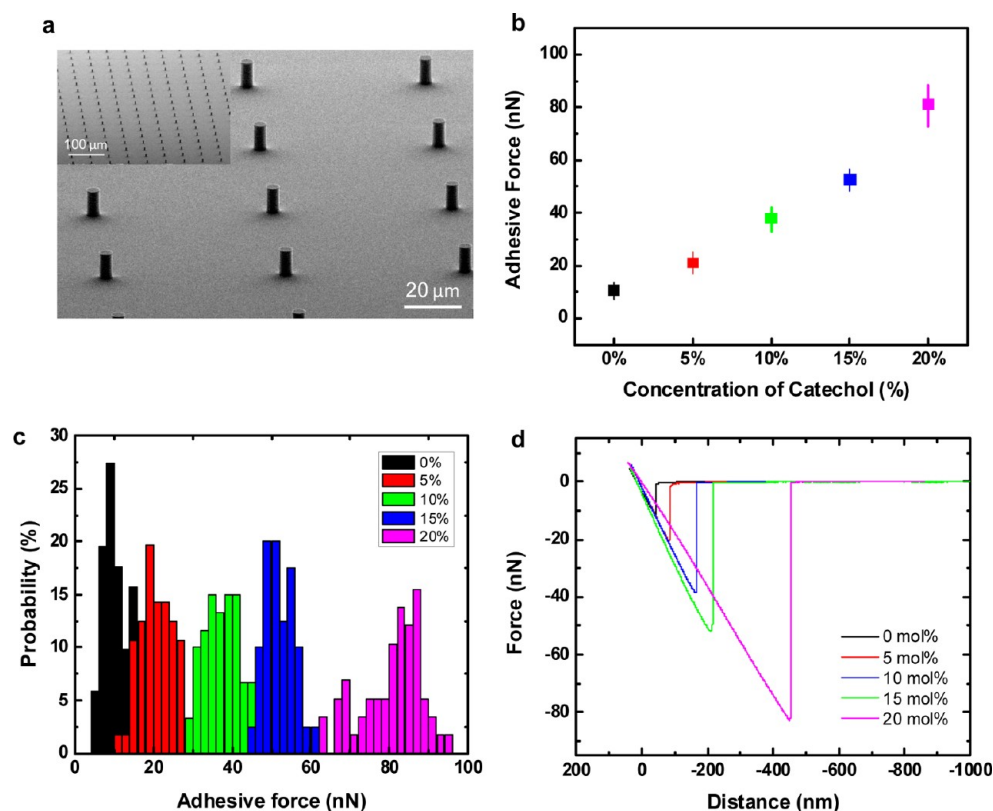


**Figure 3.** Measurement of adhesive force for fabricated microstructures based on catechol-functionalized polysiloxanes after deprotection. (a) SEM images of fabricated microstructures ( $5\ \mu\text{m}$  diameter,  $10\ \mu\text{m}$  height, 2:1 aspect ratio). (b) Plot of adhesive force vs concentration of catechol units in the starting polysiloxane. (c) Histogram of adhesive force vs concentration of catechol units in the starting polysiloxane. (d) Representative force–distance curves of fabricated microstructures incorporating different concentrations of catechol from 0 to 20 mol %.

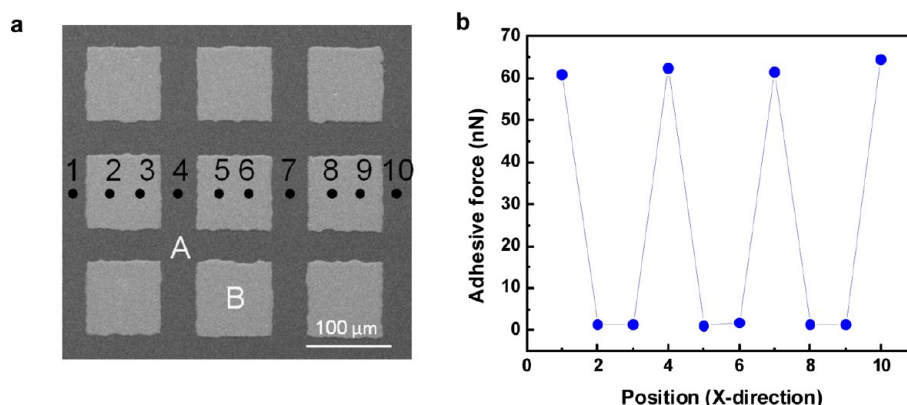


**Figure 4.** (a) SEM image of a patterned catechol-functionalized polysiloxane film: (A) catechol-functionalized polysiloxane areas; (B) Ti/Au metal-coated areas. (b) Measured adhesive force vs position on the wafer.

the contact adhesion of a single pillar would be measured. Figure 3a shows a representative scanning electron microscopy (SEM) image of the fabricated microstructures based on SPC-functionalized polysiloxane-based materials with a pillar diameter of  $5\ \mu\text{m}$  and a height of  $10\ \mu\text{m}$  (2:1 aspect ratio).

To demonstrate the ability to fabricate microstructures with photocured SPC-functionalized polysiloxane-based materials while retaining and tuning their adhesive properties, surface forces were measured in aqueous solutions using an AFM system coupled with a tipless cantilever ( $\text{Si}_3\text{N}_4$ ). The cantilever was coated with a 10 nm thick layer of  $\text{TiO}_2$  by e-beam evaporation of Ti followed by  $\text{O}_2$  plasma treatment. The oxide surface then provided specific and reversible binding with the

catecholic moieties on the surface of the photocured SPC-functionalized microstructures/films.<sup>54</sup> After the  $\text{TiO}_2$  coating was applied, the spring constant of each cantilever was calibrated on the basis of its thermal vibration factor before it was used to measure adhesive force. In a typical adhesion experiment, the tipless cantilever first approached the wet surface of the film/microstructure, and then the retracting force was measured as a function of extension during separation. The force measurements were performed in aqueous solution buffered at pH 3.0 in order to deprotect the SPC units at the surface of the photocured polysiloxane-based films.

Following initial experiments with microstructures having different contact areas (i.e., 5, 10, 20, and  $50\ \mu\text{m}$  diameter



pillars), it was determined that 5  $\mu\text{m}$  pillars were best suited for the measurable range of adhesion values based on the AFM strategy described above (see Supplementary Figure S6). In addition, to demonstrate the correlation between the adhesive force and the concentration of catecholic moieties, five different concentrations (0, 5, 10, 15, and 20 mol %) of silyl-protected catecholic moieties were examined. Significantly, the mean values and standard deviations of single-pillar adhesive forces were found to vary from 9.8 to 83 nN as the concentration of catechol was varied from 0 to 20 mol % (Figure 3b,c). The linear relationship between adhesive force and concentration of catechol units clearly demonstrates the power of this strategy to synthesize and functionalize the surface of cross-linked films with a defined number of catechol moieties in order to modulate physical properties, analogous to marine organisms and the various proteins they produce.<sup>17</sup> The representative force–distance curve is shown in Figure 3d, in which the adhesive force was determined from an average of 60 curves.

To demonstrate further the utility of SPCs as building blocks for adhesive materials, continuous polysiloxane-based films were patterned by coating with metal (Au on Ti) films deposited by e-beam evaporation using transmission electron microscopy (TEM) grids as a shadow mask. Figure 4a shows an SEM image of a patterned polysiloxane/metal film, in which dark regions (A) are the thiol–ene-derived films with catecholic moieties and bright regions (B) are the areas covered with evaporated metal. As the tipless AFM cantilever was moved across the surface, a dramatic change in adhesive force was observed as the surface changed from catechol (ca. 60 nN) to metal (<5 nN), exactly correlating with the patterned areas (Figure 4b). This is a further indication of the specific and reversible interaction of the oxide cantilever surface with the catechol groups. While these results were obtained using thin films containing 15% catechol groups, it should be noted that similar differential adhesion was observed for other patterned films with different catechol loadings. These results also demonstrate the versatility and robustness of SPC moieties, as the adhesive properties of the final films were not changed during micropatterning, which employed harsh metal deposition techniques. Attempts to perform the same experiments with unprotected catechol groups or after deprotection of the SPC units were not successful, presumably because the catechol units underwent unwanted oxidation/side reactions during patterning, processing, or deposition.

The tunable building-block nature of the materials described above, coupled with the oxidative stability of the silyl-protected catechol groups, now permits a wide range of formats and functions to be developed for these systems, which in turn allow control over macroscopic properties such as adhesion. To illustrate these features, applications of these materials as bioinspired underwater adhesives and as active surfaces for capturing/retaining oxide particles were investigated.

A simple, quantitative strategy was therefore developed through a combination of soft-imprint lithography<sup>55</sup> and transfer printing<sup>56,57</sup> to investigate the 3D assembly and adhesion of microparticle-based oxide superstructures. The design of these experiments allowed many aspects of the power of this protected catechol strategy to be illustrated, such as the stability of the SPC units during processing and 3D fabrication and the ability to control the assembly of complex microstructures through predefined adhesion properties.<sup>58</sup> It should also be noted that this 3D assembly strategy represents a variation of the recent subtractive patterning via chemical lift-off

lithography developed by Weiss and Andrews. In this strategy, strong reversible interactions (catechol–oxide) are exploited for lift-off in comparison with covalent (Si–O) bonding.<sup>59</sup> As shown schematically in Figure 5, arrays of microstructured

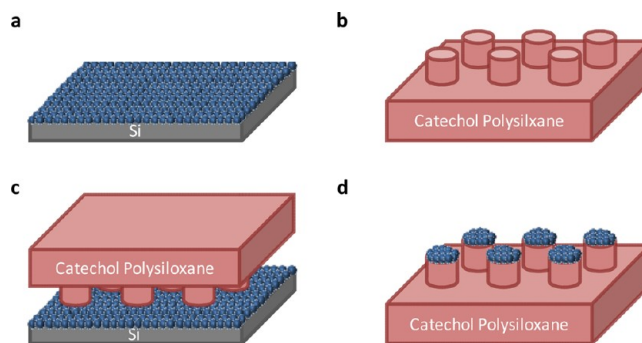


**Figure 5.** General strategy for qualitative testing of the adhesion of silica particles to functionalized siloxane-based micropillars. (a) Preparation of silica-particle-coated Si substrate. (b) Fabrication of SPC-functionalized polysiloxane-based microstructures and activation of catechol. (c) Stamping of activated catechol-functionalized polysiloxane-based microstructures on coated silica particles. (d) Removal of the catechol-functionalized polysiloxane-based film from the Si substrate.

pillars were brought into contact with oxide particles supported on a solid substrate, and as a result of the lower modulus of the polymeric pillars, these particles were transferred to the tops of the pillars after lift-off. Sonication and extensive washing then provided a quantitative analysis of the adhesion between the particle and the pillar. First, arrays of pillars (10  $\mu\text{m}$  diameter  $\times$  20  $\mu\text{m}$  height; Figure 6b) were prepared using SPC-functionalized polysiloxanes with a 20% catechol loading. The silyl protecting groups were then removed by acidic hydrolysis, and a layer of silica particles was transferred to the top surface (Figure 6c). As a control, the same assembly was fabricated using pillars from which the silyl protecting groups were not removed (Figure 6d). Significantly, after sonication and washing of the surfaces, the silica particles remained strongly attached to the tops of the pillars only in the case of the deprotected materials, where there was a direct interaction between the oxide surface of the particles and the catechol units of the pillars (Figure 6e). In direct contrast, the silica particles were easily and completely dislodged from the tops of the pillars made using the silyl-protected system (Figure 6f).

A further demonstration of the biomimetic nature of this system was obtained from the fabrication of metal oxide particle assemblies on the surfaces of flexible films. In this example, continuous films were prepared from the SPC-functionalized polysiloxane-based thiol–ene mixture followed by photo-cross-linking, and the silica particles were transferred by contact printing between an “inked” conventional polydimethylsiloxane (PDMS) elastomeric stamp and the adhesive surface. With this approach, various patterns of silica microparticles were easily assembled on the adhesive catechol surfaces (Figure 7) with strong anchoring that resisted washing and sonication.

## CONCLUSION

The importance of silyl protection in the synthesis, processing, and utilization of catechol-based materials has been demonstrated through the development of a facile and efficient strategy for the preparation of polysiloxane derivatives. These

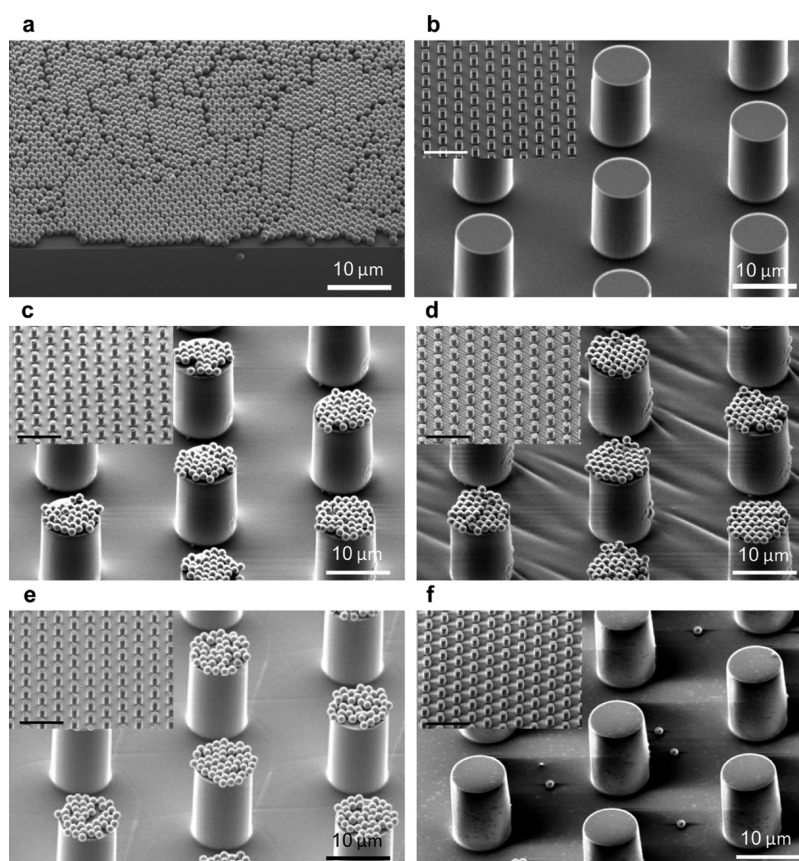


**Figure 6.** Representative SEM images demonstrating the adhesive capabilities of the fabricated catechol microstructures with silica particles. (a) Silica particles (1  $\mu\text{m}$  diameter) employed in the experiments. (b) Fabricated catechol microstructures (10  $\mu\text{m}$  diameter  $\times$  20  $\mu\text{m}$  height). (c) Silica particles directly transferred to the tops of catechol-functionalized pillars. (d) Silica particles directly transferred to tops of SPC-functionalized pillars. (e) Strong adhesion demonstrated by the stability of assembled silica particles on catechol-functionalized pillars after sonication and extensive washing. (f) Loss of adhesion for SPC-functionalized pillars after sonication and extensive washing. Scale bars in small insets of (b–f) are 50  $\mu\text{m}$ .

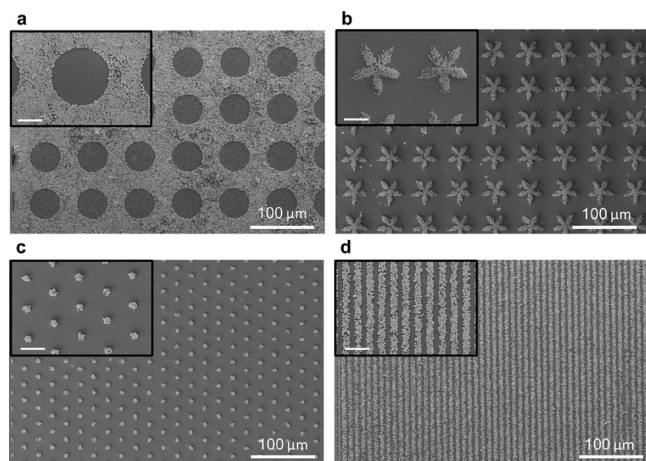


**Figure 7.** Representative SEM images of assemblies formed after transfer printing using micrometer-sized silica particles: (a) 50  $\mu\text{m}$  diameter circles; (b) 50  $\mu\text{m}$  flower shapes in a square lattice; (c) 7  $\mu\text{m}$  diameter circles in a hexagonal lattice; (d) 5  $\mu\text{m}$  line and space patterns. Scale bars in small insets of (a–d) are 20  $\mu\text{m}$ .

silyl-protected catechol (SPC)-functionalized polysiloxanes were fabricated into a variety of 2D and 3D patterned surfaces using thiol–ene chemistry with straightforward pH-activated, catechol-mediated adhesion. Significantly, the adhesion was tunable by simply increasing or decreasing the concentration of protected catechol units along the polysiloxane backbone. A

key feature of these SPC-functionalized materials is their oxidative stability, which is not affected by processing or fabrication procedures and provides long shelf life under ambient conditions. The user-friendly nature of their synthesis and subsequent activation chemistry makes these SPC-functionalized polysiloxanes a promising and versatile new platform for underwater surface treatments, including paints, coatings, adhesive tapes, and glues.

## ■ ASSOCIATED CONTENT

### 📄 Supporting Information

Complete experimental procedures along with additional supporting data. This material is available free of charge via the Internet at <http://pubs.acs.org>.

## ■ AUTHOR INFORMATION

### Corresponding Author

[hawker@mrl.ucsb.edu](mailto:hawker@mrl.ucsb.edu)

### Author Contributions

○J.H. and T.K. contributed equally.

### Notes

The authors declare no competing financial interest.

## ■ ACKNOWLEDGMENTS

This material is based upon work supported by the National Science Foundation (MRSEC Program, DMR-1121053, supporting J.H., T.K., J.M.S., J.H.W., and C.J.H.). This work



was also partially supported by the Institute for Collaborative Biotechnologies through Grants W911NF-07-1-0279 and W911NF-09-D-0001 from the U.S. Army Research Office (S.G.J., K.L.K., and C.J.H.), the National Institutes of Health (R01 DE018468 to J.H.W.), and fellowship support from Samsung (to T.K.).

## REFERENCES

- (1) Capadona, J. R.; Shanmuganathan, K.; Tyler, D. J.; Rowan, S. J.; Weder, C. *Science* **2008**, *319*, 1370–1374.
- (2) Cho, Y.; Sundaram, H. S.; Finlay, J. A.; Dimitriou, M. D.; Callow, M. E.; Callow, J. A.; Kramer, E. J.; Ober, C. K. *Biomacromolecules* **2012**, *13*, 1864–1874.
- (3) Aida, T.; Meijer, E. W.; Stupp, S. I. *Science* **2012**, *335*, 813–817.
- (4) Miesch, C.; Kosif, I.; Lee, E.; Kim, J.-K.; Russell, T. P.; Hayward, R. C.; Emrick, T. *Angew. Chem., Int. Ed.* **2012**, *51*, 145–149.
- (5) Waite, J. H. *Integr. Comp. Biology* **2002**, *42*, 1172–1180.
- (6) Wiegmann, M. *Aquat. Sci.* **2005**, *67*, 166–176.
- (7) Silverman, H. G.; Roberto, F. F. *Mar. Biotechnol.* **2007**, *9*, 661–681.
- (8) Waite, J. H.; Tanzer, M. L. *Science* **1981**, *212*, 1038–1040.
- (9) Waite, J. H.; Tanzer, M. L. *Biochem. Biophys. Res. Commun.* **1980**, *96*, 1554–1561.
- (10) Waite, J. H. *Int. J. Biol. Macromol.* **1990**, *12*, 139–144.
- (11) Zeng, H.; Hwang, D. S.; Israelachvili, J. N.; Waite, J. H. *Proc. Natl. Acad. Sci. U.S.A.* **2010**, *107*, 12850–12853.
- (12) Holten-Andersen, N.; Harrington, M. J.; Birkedal, H.; Lee, B. P.; Messersmith, P. B.; Lee, K. Y. C.; Waite, J. H. *Proc. Natl. Acad. Sci. U.S.A.* **2011**, *108*, 2651–2655.
- (13) Haeshin, L.; Dellatore, S. M.; Miller, W. M.; Messersmith, P. B. *Science* **2007**, *318*, 426–430.
- (14) Ling, D.; Park, W.; Park, Y. I.; Lee, N.; Li, F.; Song, C.; Yang, S.-G.; Choi, S. H.; Na, K.; Hyeon, T. *Angew. Chem., Int. Ed.* **2011**, *50*, 11360–11365.
- (15) Sun, C. J.; Waite, J. H. *J. Biol. Chem.* **2005**, *280*, 39332–39336.
- (16) Harrington, M. J.; Masic, A.; Holten-Andersen, N.; Waite, J. H.; Fratzl, P. *Science* **2010**, *328*, 216–220.
- (17) Waite, J. H.; Andersen, N. H.; Jewhurst, S.; Sun, C. J. *J. Adhes.* **2005**, *81*, 297–317.
- (18) Polmanteer, K. E. *Rubber Chem. Technol.* **1988**, *61*, 470–502.
- (19) Quinn, K. J.; Courtney, J. M. *Br. Polym. J.* **1988**, *20*, 25–32.
- (20) Voronkov, M. G.; Milenshkevich, V. P.; Yuzhelevskii, Y. A. *The Siloxane Bond*; Consultants Bureau: New York, 1978.
- (21) Noll, W. *Chemistry and Technology of Silicones*; Academic Press: New York, 1968.
- (22) Abbasi, F.; Mirzadeh, H.; Katbab, A. A. *Polym. Int.* **2001**, *50*, 1279–1287.
- (23) Yilgor, I.; McGrath, J. E. *Advances in Organosiloxane Copolymers*; Springer: Berlin, 1988.
- (24) Lee, H.; Lee, B. P.; Messersmith, P. B. *Nature* **2007**, *448*, 338–341.
- (25) Yu, J.; Wei, W.; Danner, E.; Israelachvili, J. N.; Waite, J. H. *Adv. Mater.* **2011**, *23*, 2362–2366.
- (26) Yu, J.; Wei, W.; Danner, E.; Ashley, R. K.; Israelachvili, J. N.; Waite, J. H. *Nat. Chem. Biol.* **2011**, *7*, 588–590.
- (27) Blackwell, J. M.; Foster, K. L.; Beck, V. H.; Piers, W. E. *J. Org. Chem.* **1999**, *64*, 4887–4892.
- (28) Chojnowski, J.; Rubinsztajn, S.; Cella, J. A.; Fortuniak, W.; Cypriak, M.; Kurjata, J.; Kazmierski, K. *Organometallics* **2005**, *24*, 6077–6084.
- (29) Chojnowski, J.; Fortuniak, W.; Kurjata, J.; Rubinsztajn, S.; Cella, J. A. *Macromolecules* **2006**, *39*, 3802–3807.
- (30) Thompson, D. B.; Brook, M. A. *J. Am. Chem. Soc.* **2008**, *130*, 32–33.
- (31) Rubin, M.; Schwier, T.; Gevorgyan, V. *J. Org. Chem.* **2002**, *67*, 1936–1940.
- (32) Blackwell, J. M.; Sonmor, E. R.; Scoccitti, T.; Piers, W. E. *Org. Lett.* **2000**, *2*, 3921–3923.
- (33) Ishihara, K.; Yamamoto, H. *Eur. J. Org. Chem.* **1999**, 527–538.
- (34) Blackwell, J. M.; Morrison, D. J.; Piers, W. E. *Tetrahedron* **2002**, *58*, 8247–8254.
- (35) Gevorgyan, V.; Rubin, M.; Benson, S.; Liu, J. X.; Yamamoto, Y. *J. Org. Chem.* **2000**, *65*, 6179–6186.
- (36) Erker, G. *Dalton Trans.* **2005**, 1883–1890.
- (37) Roesler, R.; Har, B. J. N.; Piers, W. E. *Organometallics* **2002**, *21*, 4300–4302.
- (38) Piers, W. E.; Chivers, T. *Chem. Soc. Rev.* **1997**, *26*, 345–354.
- (39) Killops, K. L.; Campos, L. M.; Hawker, C. J. *J. Am. Chem. Soc.* **2008**, *130*, 5062–5064.
- (40) Campos, L. M.; Killops, K. L.; Sakai, R.; Paulusse, J. M. J.; Dameron, D.; Drockenmuller, E.; Messmore, B. W.; Hawker, C. J. *Macromolecules* **2008**, *41*, 7063–7070.
- (41) Gress, A.; Volkel, A.; Schlaad, H. *Macromolecules* **2007**, *40*, 7928–7933.
- (42) Justynska, J.; Schlaad, H. *Macromol. Rapid Commun.* **2004**, *25*, 1478–1481.
- (43) David, R. L. A.; Kornfield, J. A. *Macromolecules* **2008**, *41*, 1151–1161.
- (44) ten Brummelhuis, N.; Diehl, C.; Schlaad, H. *Macromolecules* **2008**, *41*, 9946–9947.
- (45) Hoyle, C. E.; Lee, T. Y.; Roper, T. J. *Polym. Sci., Part A: Polym. Chem.* **2004**, *42*, 5301–5338.
- (46) Cole, M. A.; Bowman, C. N. *J. Polym. Sci., Part A: Polym. Chem.* **2012**, *50*, 4325–4333.
- (47) Lo Conte, M.; Robb, M. J.; Hed, Y.; Marra, A.; Malkoch, M.; Hawker, C. J.; Dondoni, A. *J. Polym. Sci., Part A: Polym. Chem.* **2011**, *49*, 4468–4475.
- (48) Kang, T.; Amir, R. J.; Khan, A.; Ohshimizu, K.; Hunt, J. N.; Sivanandan, K.; Montanez, M. I.; Malkoch, M.; Ueda, M.; Hawker, C. J. *Chem. Commun.* **2010**, 46, 1556–1558.
- (49) Amir, R. J.; Albertazzi, L.; Willis, J.; Khan, A.; Kang, T.; Hawker, C. J. *Angew. Chem., Int. Ed.* **2011**, *50*, 3425–3429.
- (50) Campos, L. M.; Meinel, I.; Guino, R. G.; Schierhorn, M.; Gupta, N.; Stucky, G. D.; Hawker, C. J. *Adv. Mater.* **2008**, *20*, 3728–3733.
- (51) Xu, T.; Stevens, J.; Villa, J. A.; Goldbach, J. T.; Guarim, K. W.; Black, C. T.; Hawker, C. J.; Russell, T. R. *Adv. Funct. Mater.* **2003**, *13*, 698–702.
- (52) Barner-Kowollik, C.; Du Prez, F. E.; Espeel, P.; Hawker, C. J.; Junkers, T.; Schlaad, H.; Van Camp, W. *Angew. Chem., Int. Ed.* **2011**, *50*, 60–62.
- (53) Waite, J. H.; Qin, X. X. *Biochemistry* **2001**, *40*, 2887–2893.
- (54) Lee, H.; Scherer, N. F.; Messersmith, P. B. *Proc. Natl. Acad. Sci. U.S.A.* **2006**, *103*, 12999–13003.
- (55) Odom, T. W.; Love, J. C.; Wolfe, D. B.; Paul, K. E.; Whitesides, G. M. *Langmuir* **2002**, *18*, 5314–5320.
- (56) Meitl, M. A.; Zhu, Z. T.; Kumar, V.; Lee, K. J.; Feng, X.; Huang, Y. Y.; Adesida, I.; Nuzzo, R. G.; Rogers, J. A. *Nat. Mater.* **2006**, *5*, 33–38.
- (57) Park, J.; Hammond, P. T. *Adv. Mater.* **2004**, *16*, S20–S25.
- (58) Kim, T.-H.; Cho, K.-S.; Lee, E. K.; Lee, S. J.; Chae, J.; Kim, J. W.; Kim, D. H.; Kwon, J.-Y.; Amaratunga, G.; Lee, S. Y.; Choi, B. L.; Kuk, Y.; Kim, J. M.; Kim, K. *Nat. Photonics* **2011**, *5*, 176–182.
- (59) Liao, W. S.; Cheunkar, S.; Cao, H. H.; Bednar, H. R.; Weiss, P. S.; Andrews, A. M. *Science* **2012**, *337*, 1517–1521.